Posters Session I – B
Nanomaterials Characterization / Properties and Tools

Study of chairlity by High Resolution Optical Microscope of Si-CNT Prepared by Plasma Sputtering without catalyst

Bassam M. Mustafa, Anwar M. Ezzat and Mohammad M. Uonis
Department of Physics, College of Science, Mosul University, Mosul, Iraq

Abstract: Fabrication of Si-CNT (silicon- carbon nano tube) junction is done by plasma sputtering of Carbon from graphite rods in Argon gas atmosphere, without catalysts for thicknesses 10 – 82 nanometer . Study of images of the specimen by Scanning electron microscope shows that the carbon layer is in the form carbon nanotubes with diameters about 30 nanometer The Raman, x-ray and the energy dispersive x-ray (EDXR) spectra shows peaks characteristics of the carbon nanotubes . More careful study of the carbon layer surface by high resolution optical microscope is done using both transmission and reflection methods , then images are amplified more by computer software .The transmission images for carbon layer on the glass substrate shows two dimensional nanotubes structures . Images taken by reflection of white light from the carbon layer on Si-C junction, shows clearly zigzag nanotubes chairlity The I-V measurements using gold electrodes shows semiconducting behavior ensuring the zigzag chairlity .

Keywords: Carbon nanotubes, Plasma sputtering, Si-C junction, chairlity.

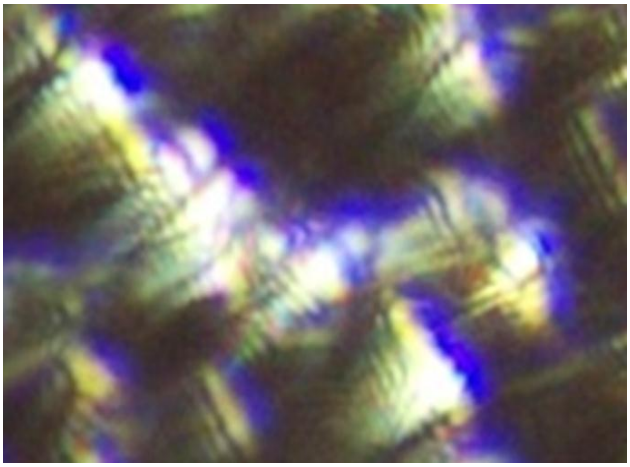

Figure 1: show the images for carbon nano layers deposited on silicon wafer taken by high resolusion light microscope with a digital camera after magnification by 850% by computer software.

References:

Uonis, M. , Mustafa, B. and Ezzat, A. (2014) The Role of Sputtering Current on the Optical and Electrical Properties of Si-C Junction. World Journal of Nano Science and Engineering, 4,90-96.
doi: 10.4236/wjnse.2014.42012.

Uonis, M. , Mustafa, B. and Ezzat, A. (2014) The Effect of Carbon Rod—Specimens Distance on the Structural and Electrical Properties of Carbon Nanotube. World Journal of Nano Science and Engineering, 4,105-110.
doi:10.4236/wjnse.2014.43014.

Gas-Generating Theranostic Nanoparticles for Ultrasound Imaging and Photodynamic Therapy

D. J. Park,[1] K. H. Min,[1] S. C. Lee[2,*]
[1]Department of Life and Nanopharmaceutical Science, College of Pharmacy, Kyung Hee University, Seoul, Republic of Korea
[2]Department of Maxillofacial Biomedical Engineering, School of Dentistry, Kyung Hee University, Seoul, Republic of Korea

Abstract: Recently, theranostic nanoparticles, which integrate imaging and therapeutic functionalities, have played a central role in the improvement of tumor treatment. In this work, we develop a gas-generating calcium carbonate ($CaCO_3$) mineralized nanoparticle ($CaCO_3$-MNPs) that can generate carbon dioxide (CO_2) bubbles and trigger the release of photosensitizers in response to tumoral acidic pH for ultrasound (US) imaging and simultaneous therapy of tumors. To visualize CO_2 generation, in vitro contrast-enhanced ultrasound imaging and quantitative analysis of CO_2 amounts were investigated at various pH values. In vitro phototoxicity and singlet oxygen generation experiments were carried out in order to verify photodynamic effect of the photosensitizer from the nanoparticles. This work suggests that $CaCO_3$ mineralized photosensitizer-encapsulated nanoparticles can serve as theranostic nanoparticles for US imaging-guided photodynamic therapy.

Keywords: calcium carbonate, photosensitizer, mineralization, ultrasound imaging, theranostics, photodynamic therapy

As llustrated in Figure 1, we prepared Ce6-loaded mineralized nanoparticles by poly(ethylene glycol)-b-poly(L-aspartic acid) (PEG-PAsp)-mediated $CaCO_3$ mineralization in the presence of calcium cations, carbonate anions, and a negatively charged photosensitizer, chlorin e6 (Ce6). TEM images indicated that the nanoparticles had a spherical shape and a mean diameter of 300 nm. To visualize CO_2 generation from dissolved $CaCO_3$ in tumoral acidic pH, in vitro contrast-enhanced ultrasound image and quantitative analysis of CO_2 amounts were investigated at various pH. In vitro experiments showed that the $CaCO_3$-MNPs generated strong echogenic signals at tumoral pH (6.4) due to CO_2 bubble generation, whereas, at pH 7.4, there was no noticeable US contrast signals (Figure 2). In vitro phototoxicity and singlet oxygen generation experiments were carried out in order to verify photodynamic effect of Ce6 from mineralized nanoparticles. The $CaCO_3$-MNPs effectively released Ce6 at pH 6.4, and expressed the effective photodynamic therapeutic activity for MCF-7 breast cancer cells.

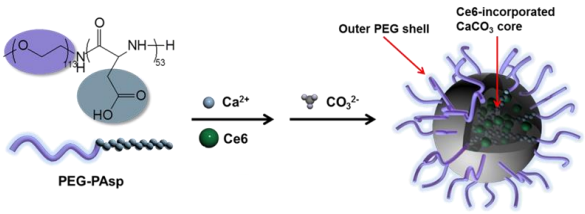

Figure 1. Fabrication of Ce6-loaded $CaCO_3$ mineralized nanoparticles through PEG-PAsp-mediated mineralization.

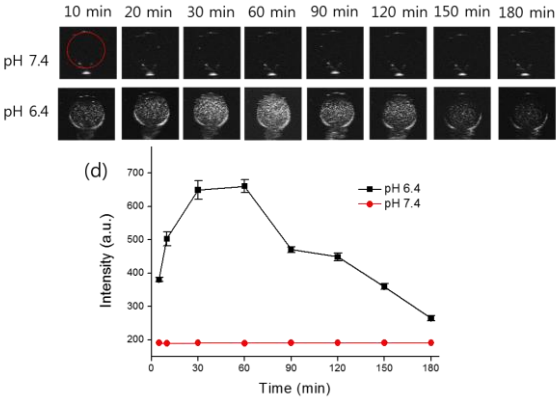

Figure 2. pH-Dependent in vitro US imaging profiles as a function of time.

References:

Rim, H. P., Min, K. H., Lee, H. J., Jeong, S. Y., Lee, S. C. (2011) pH-Tunable calcium phosphate covered mesoporous silica nanocontainers for intracellular controlled release of guest drugs, *Angew. Chem. Int. Ed.*, 50, 8853-8857.

Min, K. H., Lee, H. J., Kim, K., Kwon, I. C., Jeong, S. Y., Lee, S. C. (2012), The tumor accumulation and therapeutic efficacy of doxorubicin carried in calcium phosphate-reinforced polymer nanoparticles, *Biomaterials*, 33, 5788-5797.

Min, K. H., Min. H. S., Lee, H. J., Park, D. J., Yhee, J. Y., Kim, K., Kwon. I. C., Jeong, S. Y., Silvestre, O. F., Chen, J., Hwang, Y.-S., Kim, E.-C., Lee, S. C. pH-Controlled Gas-Generating Mineralized Nanoparticles: A Theranostic Agent for Ultrasound Imaging and Therapy of Cancers, *ACS Nano*, In Press.

The application of ultrasonic spectroscopy to the study of the gelation and chain relaxation properties of dually crosslinked hydrogels

K. Khouzami*, C. Branca, C. Crupi, S. Rifici, G. Ruello, U. Wanderlingh, G. D'Angelo
Dipartimento di Fisica e Scienze della Terra, Università di Messina, Viale S. D'Alcontres 31 98166 Messina

Abstract: One strategy to create chemical and physical cross-links simultaneously is to introduce into the chemical network hydrogen bonding with clay nanofillers. Understanding the gelation process and relaxation mechanisms of these systems is crucially important for predicting hydrogel performances in terms of degree of swelling and viscoelastic properties.

In this study, ultrasonic spectroscopy has been used to investigate the gelation kinetics and chain-relaxation properties of glutaraldehyde-cross-linked chitosan and chitosan- montmorillonite nanocomposite hydrogels.

Low intensity ultrasound was applied to the investigated systems. By measuring the amplitude of the wave in the pulse, the ultrasonic velocity and attenuation at frequencies between 5 and 25 MHz and at room temperature were determined simultaneously as a function of the time.

In all the investigated samples, we observed that the kinetics of gelation consist of two stages; a pre-gelation, indicated by fast increase in the ultrasound velocity and attenuation, and a gelation, that is revealed by inflection in the ultrasound velocity and attenuation trends.

The increase of the ultrasound attenuation is due to the viscous losses, while the increases in the ultrasonic velocity reflects the increase in the longitudinal modulus of the sample due to the contribution of the gel network.

The effects of the cross-linker and clay concentration on the hydrogel acoustic behavior have been also analysed and correlated with the elastic response of the systems.

The results demonstrate the reliability of ultrasonic spectroscopy in describing in details the network formation processes. If used in parallel with other tecniques, such as rheology and light scattering, it should help us to better understand the viscoelastic processes associated with the physical or chemical gelation and the crosslinking in hydrogel systems.

Keywords:
biomaterials, nanoporous hydrogels, polysaccharide, crosslinking, viscoelasticity, ultrasonic spectroscopy.

New challenges in TiO_2 nanoparticle characterisation and separation by Flow Field Fractionation

J. Omar, A. Boix, C. von Holst

European Commission, Joint Research Centre, Institute for Reference Materials and Measurements (EC-JRC-IRMM), Retieseweg 111, 2440 Geel, Belgium

Titanium dioxide is a widely used additive which can appear in a broad variety of final products such as paint pigments, toothpastes, sunscreens, coffee creamers, food colorants, etc. due to its different properties. The European Commission's Joint Research Centre (JRC) established a repository with Representative Test Materials (RTMs) consisting of different types of particulate nanomaterials, from which three titanium dioxide materials were chosen for this study: NM 101, NM 102 and NM 104. All the materials presented a different particle size (mean particle size 38, 132 and 67 nm respectively), the first two RTMs are known as anatase mineral and the last RTM as rutile.

The aim of this study was to develop a separation and characterisation method for each of the chosen RTMs by means of Field Flow Fractionation (FFF) system. In a first approach, the most suitable dispersant and eluent were chosen for each of the RTMs among them water, sodium pyrophosphate, Novachem and BSA. Next, the FFF system was optimized for each material employing experimental design: the tip flow, cross flow, detector flow and focusing time were studied. Concerning the sample preparation, the use of Focused Ultrasound Systems is becoming more and more necessary, however, the impact of the ultrasounds (time and amplitude) in the RTM was also studied by means of Experimental Design.

Diamagnetism of Superparamagnetic Ni Nanoparticles Incapsulated in Carbon Shells

A. Manukyan,[1*] A. Mirzakhanyan,[1] H. Gyulasaryan,[1] M. Farle,[2] E. Sharoyan[1]
[1]Institute for Physical Research, NAS of Armenia, Laboratory of Solid State Physics, Ashtarak-2, Armenia
[2] Universität Duisburg-Essen, Fakultät für Physik and Center for Nanointegration, Duisburg, Germany

Abstract: Using the method of solid-phase pyrolysis of solid solutions of nickel phthalocyanine – metal-free phthalocyanine, $\{(NiPc)_x(H_2Pc)_{1-x}$, $0<x<1\}$, we prepared single-domain ferromagnetic and superparamagnetic Ni nanoparticles coated by graphite-like shells, i.e. Ni@C nanocomposites. A considerable diamagnetism was observed in case of ultrafine Ni nanoparticles when their mean size, d_m, was less than 17 nm.

The dependence is shown in Figure 1 of the total and diamagnetic parts of the magnetization of Ni@C nanocomposites upon external magnetic field at 300K. The values of the concentration, c, of Ni in carbon were equal to 0; 0.5; 0.75; and 2.5 at % and the values of diamagnetic susceptibility were -1×10^{-6}; -3×10^{-5}; -2×10^{-5}; and -6×10^{-6} emu/(g·Oe) correspondingly. The diamagnetism in Ni-containing samples is substantially higher as compared to that of the carbon matrix $\chi^{dia}(c=0.5) = 30\chi^{dia}(c=0)$. Unfortunately, it is not possible to compare the diamagnetism of Ni@C nanocomposites with that of bulk Ni samples since no data exists about diamagnetism of bulk Ni. Evdently, the ferromagnetic magnetization in bulk Ni is so strong that it makes it impossible to observe the diamagnetic magnetization. The observation of diamagnetism in ferromagnetic metals becomes possible in case of small nanoparticles in superparamagnetic state. The paramagnetism of these nanoparticles is very low at high temperatures (100–300 K) due to $M_{para} \sim 1/T$. On the other hand our results reveal the drastic increase of diamagnetism in small metal nanoparticles. We considered possible mechanisms that can give rise to considerable diamagnetism in Ni@C nanocomposites. The "giant" diamagnetism in non-ferromagnetic nanoparticles was earlier observed in single-crystalline Au nanorods (van Rhee *et al*.; 2013).

This work was supported by the grant of Volkswagen Stiftung project A108857.

Keywords: diamagnetism in Ni nanoparticles, nickel-carbon nanocompisites, solid-phase pyrolysis, superparamagnetism.

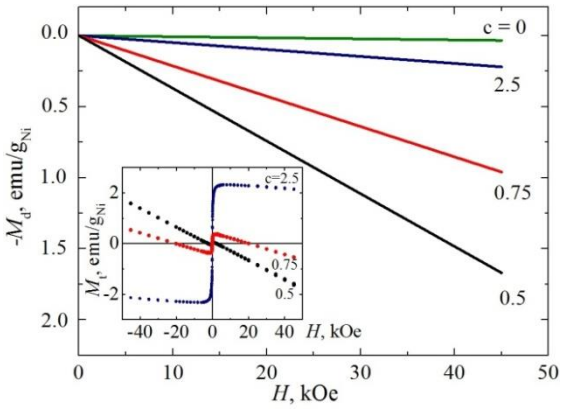

Figure 1: The dependences of the total and diamagnetic parts of the magnetization of Ni@C nanocomposites upon external magnetic field at 300 K.

References:

van Rhee, P.G., Zijlstra, P., Verhagen, T.G.A., Aarts, J., Katsnelson, M.I., Maan, J.C., Orrit, M., Christianen, P.C.M. (2013) Giant Magnetic Susceptibility of Gold Nanorods Detected by Magnetic Alignment, *Phys. Rev. Lett.*, 111, 127202.

Beryllium oxide nanowires and their optical properties for dosimetric applications

E. Pajuste*, G. Kizane, J. Prikulis, D. Erts
Institute of Chemical Physics, University of Latvia, 4 blvd. Kronvalda, Riga, LV-1586, Latvia
Phone: +371 67033883, Fax +371 67033883, E-mail: elina.pajuste@lu.lv

Abstract: Beryllium oxide is a material with a wide range of applications owing to its unusual combination of optical, thermal, dielectric and mechanical properties. Due to its high sensitivity and near tissue-equivalence beryllium oxide is used also as a OSL (optically stimulated luminescence) dosimeter[1]. It has been observed that luminescent (thermal and optical) dosimetric response of nano-phosphorus has an increased dose range with good linearity over its microcrystalline counterparts[2]. In nanostructured form dosimetric materials have a considerably higher measured dose upper limit[3]. This characteristic is of marked interest in several dosimeter applications for e.g. radiation therapy of cancer, where extremely high doses are delivered to the tumour volume, and border protection where exposure to unknown source is potentially possible. Therefore it can be expected that nanostructured beryllium oxide would have better dosimetric performance over the microcrystalline one.

Beryllium nanowires with a diameter in range from 10 – 100 nm and length of 50 μm were obtained by a high temperature oxidation process of beryllium in the atmosphere of low oxygen content. The optical properties of the nanowires were compared to that of microstructured beryllium oxide powder. Emission spectra was measured for both BeO nanowires and powder by optical stimulation with different excitation wavelengths. A significant change of photoluminiscence spectra were observed in beryllium oxide nanowires if stimulated by the ultraviolet and green excitition. Preliminary irradiation experiments with the accelerated electrons have been performed (Figure 2) and dosimetric response assessed.

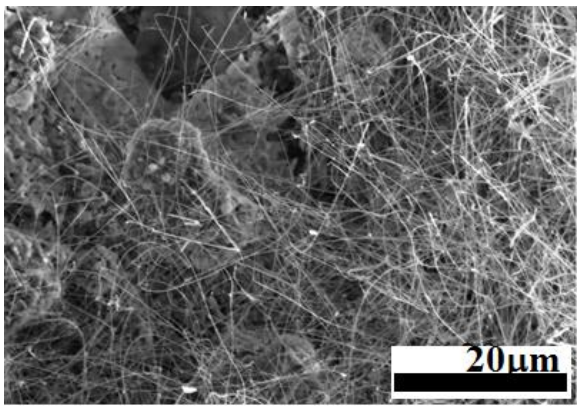

Figure 1: Beryllium oxide nanowires

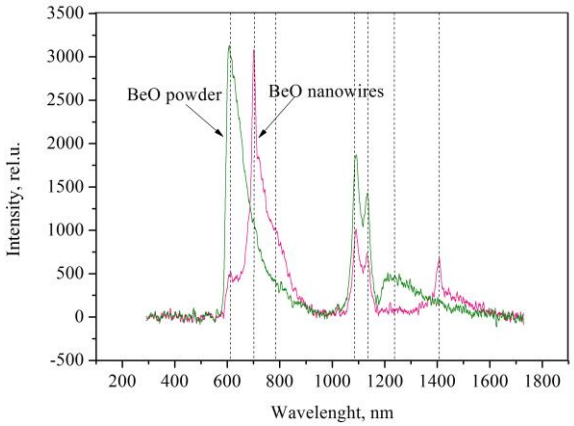

Figure 2: Photoluminiscence induced by green light excitation of BeO microcrystalline powder and nanowires after 500 Gy dose irradiation with 5 MeV accelerated electrons

This work was done within ESF project 2013/0028/1DP/1.1.1.2.0/13/APIA/VIAA/054.

References:

1. Jahn, A., M. Sommer, W. Ullrich, M. Wickert and J. Henniger (2013) The BeOmax system – Dosimetry using OSL of BeO for several applications. *Radiation Measurements*, **56**,. 324-327.
2. Kortov, V.S. (2010) Nanophosphors and outlooks for their use in ionizing radiation detection. *Radiation Measurements*,. **45**(3–6),512-515.
3. Erfani Haghiri, M., E. Saion, N. Soltani and W. SAffiey wan Abdullah (2014), Thermoluminescence Properties of Nanostructured Calcium Borate as a Sensitive Radiation Dosimeter for High Radiation Doses *Advanced Materials Research*, **832**, 189 -194.

Computer microscopy of biological liquid dry patterns for medical diagnostics and modeling of their properties by dissipative dynamics methods

P. Lebedev-Stepanov ,[1,2,*] M. Buzoverya,[3] I. Shishpor[3], K. Vlasov[2]
[1]Photochemistry Center RAS, Moscow, Russia
[2]National Research Nuclear University MEPhI, Moscow, Russia
[3] Sarov State Physics Technical Institute, Sarov, Russia

Abstract:

A number of papers devoted to heat and mass transfer into colloidal solution evaporating drops on a flat substrate have been published over the last years, mainly due to the importance of this problem for fundamental and applied sciences and technologies.
Report demonstrates some capabilities of the hardware-software complex *Morfo* in the field of solving the diagnostics problems of the human body in normal state, and when pathology states are being developed (Fig.1) [1,2]. The complex's application has allowed obtaining of interesting results not only in biomedical applications, but also acquisition of interesting data on the processes of facies structure formation**.**
Also we are elaborating the useful software complex to predictive modeling of setup, spreading, evaporation of liquid droplet of inkjet size, as well as self-assembly of solvated monodisperse nanoparticles from the drop during evaporation (Fig. 2), [3]. The most difficult case for modeling is a drop of biological liquid (such as blood serum, tear, saliva et al.) which consists of many different components of solution and forms the complex dry pattern onto substrate as a final stage of solvent evaporation process.
The modern computer methods are not yet able to model such a system in details. This study includes consideration of perspectives of further development of DPD methods to describing the formation of the dry pattern (Fig.3) which gives the new opportunities for interpretation of this process and pattern diagnostics optimization.

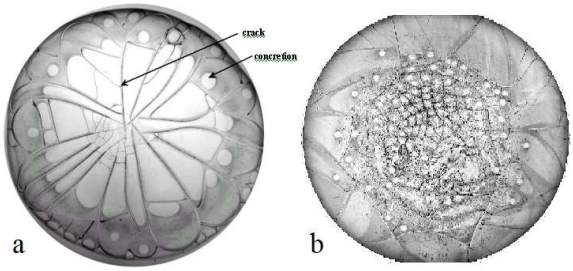

Figure 1: Blood serum facies: a – norm; b – pathology.

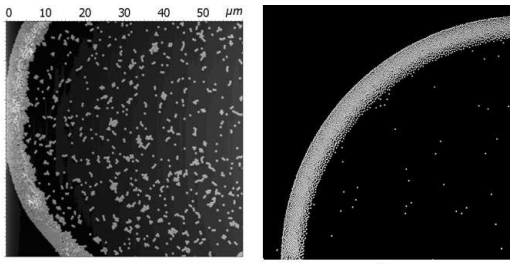

Figire 2: a - ASM image of inkjet droplet pattern which consists of monodisperse colloidal particles. b –DPD numerically modeling pattern. The calculation visualization was performed via VMD 1.8.

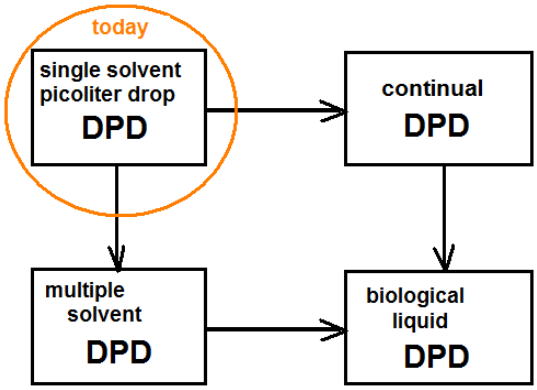

Figure 3: Running status and perspectives in modelling by dissipative particle dynamics (DPD)

Keywords: microstructural bio-liquids' analysis, quantitative microscopy, cracks, concretions, hardware-software complex, biomedical applications, dissipative particle dynamics (DPD), self-assembly, computer modeling, nanoparticles.

References:

1. Shabalin, V., Shatokhina, S. (2001), The human being bio-liquids' morphology, Moscow, Khrizostom. 304 P.
2. Buzoverya, M, Shishpor, I., Potekhina, Yu., Shcherbak, Yu. (2012), The bio-liquids' microstructural analysis, *Journal of Technical Physics*, 82, 7, 123-128.
3. Lebedev-Stepanov, P., Vlasov K. (2013), Simulation of self-assembly in an evaporating droplet of colloidal solution by dissipative particle dynamics, *Colloids and Surfaces A: Physicochem. Eng. Aspects*, 432, 132–138.

Theoretical studies on electronic and magnetic properties of a two-dimensional Mn-Pc and Mn-TCNB monolayers

M. MABROUK[1,2*], R. HAYN[1]
[1]Aix-Marseille Université, CNRS, IM2NP-UMR 7334, 13397 Marseille Cedex 20, France
[2]Laboratory for Advanced Materials and Interfaces, Faculty of Sciences of Monastir, Avenue of the Environment, 5019 Monastir, Tunisia

Abstract: The electronic and magnetic properties of a two-dimensional manganese phthalocyanine Mn-Pc monolayer and the metal-ligand network Mn-TCNB (Figure 1) are investigated by first principal calculations based on density functional theory with the inclusion of the Hubbard like-Coulomb term.
We show that both structures have a metallic behavior with a total magnetic moment of about 3 μ_B (Koudia *et al.*, 2014). We notice that a partial screening is present in the Mn-TCNB monolayer where a local moment S=5/2 at the Mn centers is reduced by unpaired electrons at the ligands. Such a picture explains the recent XMCD measurements of Mn-TCNB (Giovanelli *et al.*, 2014). Our results present theoretical insight of new metal-organic networks being important for future molecular spintronics.

Keywords: Manganese phthalocyanine, TCNB, half-metal, molecular spinctronics, Density function theory.

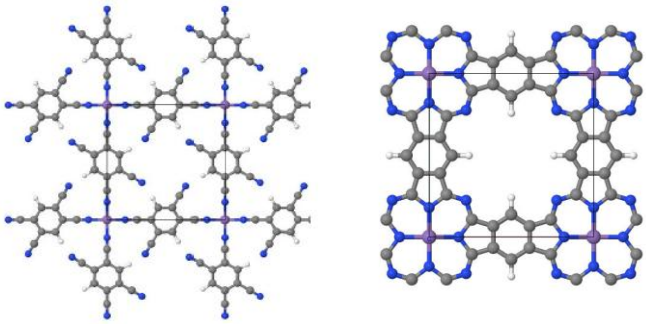

Figure 1: Structure of the 2D Mn-TCNB and Mn-Pc networks respectively. The Mn, N, C, and H atoms are highlighted in violet, blue, gray, and white, respectively. The square represent the unit cell.

References:

Giovanelli, L., Savoyant, A., Abel, M., Maccherozzi, F., Ksari, Y., Koudia, M., Hayn, R., Choueikani, F., Otero, E., Ohresser, P., Themlin, J.-M., Dhesi, S. S., Clair, S. (2014), Magnetic Coupling and Single-Ion Anisotropy in Surface-Supported Mn-Based Metal–Organic Networks, *J. Phys. Chem. C*, 118, 11738-11744.

Koudia, M., Abel, M. (2014), Step-by-step on-surface synthesis: from manganese phthalocyanines to their polymeric form, *Chem. Commun.*, 50, 8565-8567.

Band Structure of ABA-Trilayer Graphene Superlattice under the Application of Periodic Kronig-Penney Type of Potential

Salah Uddin,[1] K. S. Chan,[2*]
[1, 2*]Department of Physics and Materials Science, City University of Hong Kong

Abstract: After the discovery of graphene, theoretical physicists have been investigating methods to modify the electrical properties of massless Dirac quasiparticles. This work presents the development of a new numerical method to investigate the effect of one-dimensional periodic potential on the low energy band structure of ABA-trilayer graphene superlattice. This method can also be generalized to study multilayer graphene too. We use the Fourier transformation approach to convert the low energy continuum Hamiltonian of ABA-trilayer graphene near the Dirac point in one valley to a general ABA-trilayer graphene superlattice Hamiltonian. The electric potential is also converted to a periodic superlattice potential by applying the Fourier series. The superlattice Hamiltonian along with superlattice potential is then solved numerically and got the results which are discussed below.

We consider to different cases. (1) First we assume that all the three layers have the same potential. By increasing the barrier height of the superlattice potential and keeping the barrier and well width of the potential equal, extra Dirac points having the same electron-hole crossing energy as that of the original Dirac point are generated in the energy spectrum. These extra Dirac points emerge both from the original Dirac points as well as from the valleys developed in the energy spectrum. The symmetry of the conduction and valence band broken down by making the barrier and well width unequal. The position of the original Dirac point oscillate with periodic potential while the extra Dirac points shifted upward or downward depending on the barrier and well width. The number of extra Dirac points produce by increasing the barrier height (potential) when all the three layers have the same potential are shown in figure 1. (2) If we consider each layer has a different potential then extra Dirac points always emerges from the valleys in the spectrum. Each time two extra Dirac point emerge from each single valley so four Dirac points are generated at a particular potential. These extra Dirac points are not stable; two out of four Dirac points disappear from the spectrum by increasing the barrier height of each layer. This merging and emerging of additional Dirac points is completely different from the equal potential case. The results of different potential for each layer are similar to one discuss in (Uddin *et al.*; 2014) for ABC-trilayer graphene superlattice.

Keywords: band structure of ABA-trilayer graphene superlattice, electrical properties, superlattice potential.

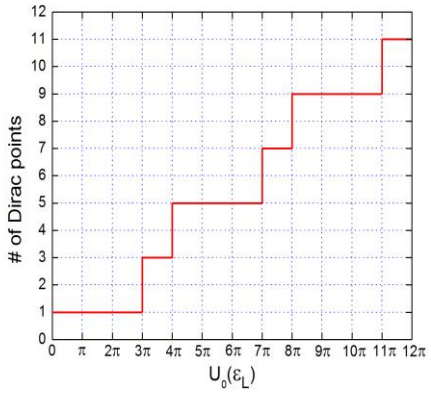

Fig. 1: Number of Dirac points (not including spin and valley degeneracies) in ABA-trilayer graphene superlattice versus barrier height.

REFERENCES

Uddin S., Chan K. S. (2014), Band structure of ABC-trilayer graphene superlattice, J. Appl. Phys. 116, 203704.

Fabrication of transparent AZO/ZnO/ITO ReRAM devices and their switching characteristics depending on the deposition temperature of ZnO active layer

K. Y. Kim,[1] C. H. Cho,[2] H. J. Kim,[2] E. L. Shim[3], and Y. J. Choi,[1]
[1] Sejong University, Department of Nanotechnology & Advanced Materials Engineering, Seoul, Republic of Korea
[2] Myongji University, Department of Physics, Gyeonggi, Republic of Korea
[3] Halla University, School of Mechanical & Automotive Engineering, Gangwon-do, Republic of Korea

Abstract: In this research, we reported the dependence of the resistive switching characteristics of transparent resistive random access memory (ReRAM) devices with AZO/ZnO/ITO structures on the deposition temperature of the ZnO active layer. During the formation of the ZnO thin film layer in the ReRAM devices, we studied the structural changes due to changes in the substrate temperature. In general, structural changes of active layers are closely related to the resistive switching characteristics of the ReRAM device. Based on the structural changes of ZnO thin film with the substrate temperature, we compared the resistive switching characteristics of the corresponding ReRAM devices. When the deposition temperature is increased, we confirmed the ZnO thin film changed properties: grain size and thin film property. In addition, the resistive switching characteristics declined. As a result, the ReRAM device with a ZnO film deposited at room temperature showed the best characteristics: forming at the lowest voltage (below 3 V), set and reset occurring between –1 V and 1 V, more than 300 cycles of endurance, and more than 10,000 s retention time.

Keywords: Resistive random access memory (ReRAM), ZnO, thin films, temperature dependence.

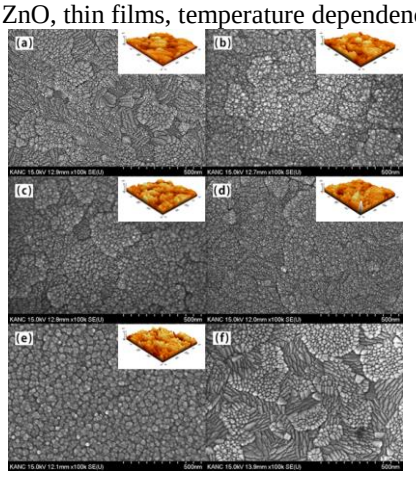

Fig. 1. (a) The SEM data of ITO thin film. The SEM data of ZnO thin film for different substrate temperatures: (b) room temperature, (c) 150℃, (d) 300℃, and (e) 450℃. (f) The ITO thin film with respect to the annealing temperature at 450℃. Insets are corresponding AFM images.

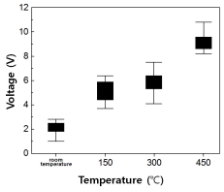

Fig. 2. Forming voltage of the ReRAM device with ITO/ZnO/AZO structure with respect to the substrate temperature.

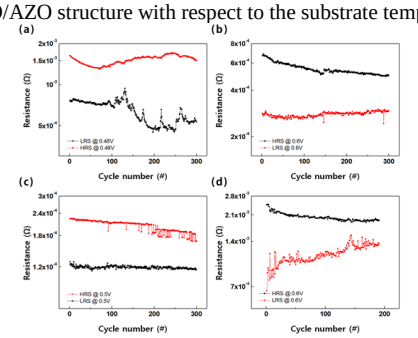

Fig. 3. Endurance of ITO/ZnO/AZO ReRAM device for different substrate temperatures: (a) room temperature, (b) 150℃, (c) 300℃, and (d) 450℃.

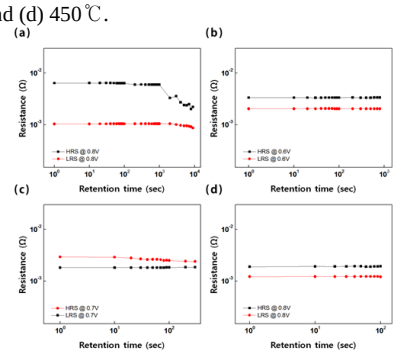

Fig. 4. Retention of the ITO/ZnO/AZO ReRAM device for different substrate temperatures: (a) room temperature, (b) 150℃, (c) 300℃, and (d) 450℃.

References:

Akinaga, H., Shima, H. (2010), Resistive Random Access Memory (ReRAM) Based on Metal Oxides, *Proceedings of the IEEE.*, 98, 2237-2251.

Xu, N., Liu, L., Sun, X., Liu, X., Han, D., Wang, Y., Han, R., Kang, J., Yu, B. (2008), Characteristics and mechanism of conduction/set process in Ti N／Zn O／Pt resistance switching random-access memories, *J. Appl. Phys.*, 92, 232112.

Singh, S., Srinivasa, R, S., Major, S, S., (2007) Effect of substrate temperature on the structure and optical properties of ZnO thin films deposited by reactive rf magnetron sputtering, *Thin Solid Films.*, 515, 8718-8722.

Physico-chemical properties of Fe-doped alumino-silicate nanotubes

E. Bahadori,[1] E. Shafia,[1] S. Esposito,[2] M. Armandi,[1] B. Bonelli,[1*]
[1] Department of Applied Science and Technology, Politecnico di Torino, Torino, Italy
[2] Department of Civil and Mechanical Engineering, Università degli Studi di Cassino, Cassino (FR), Italy

Abstract: Imogolite (IMO) is a an alumino-silicate occurring as single-walled nanotubes (NTs) with chemical formula $(OH)_3Al_2O_3SiOH$, having an outer surface made by Al-O-Al and Al(OH)Al groups and an inner surface lined by silanols (SiOH). IMO is diamagnetic and behaves as an insulator, but doping with small amount of iron could lead to new magnetic and conductive properties. Moreover, the presence of Fe sites at the outer surface of NTs, due to Fe replacing Al, could lead to interesting catalytic properties. In a previous work [1], we have investigated the synthesis of Fe-doped IMO by either direct synthesis or impregnation in basic medium so as to achieve precipitation of Fe-oxo, hydroxides. Unfortunately, the direct synthesis method proved to be very difficult, due to the presence of Fe-precursor in the synthesis medium, finally lowering the reaction yield, therefore the ionic exchange method would allow iron-doping in a simpler way.
In this work, Fe-doped NTs with an iron content of 1.4 wt. % were obtained by post-synthesis ion exchange of Imogolite ($(OH)_3Al_{2-x}Fe_xO_3SiOH$ with x = 0.05, Fex-IMO) and Methyl-Imogolite, an IMO analogous material in which inner SiOHs are replaced by $SiCH_3$ groups ($(OH)_3Al_{2-x}Fe_xO_3SiCH_3$ with x = 0.05, Fe_X-Me-IMO). Samples properties were investigated by X-ray Diffraction (XRD); N_2 sorption isotherms at 77 K and Diffuse Reflectance (DR) UV-Vis spectroscopy. The results were compared with previous research on a set of Fex-IMO samples obtained by direct synthesis and post-synthesis impregnation [1].
Evidence is given of the isomorphic substitution of Fe for Al in both Fex-IMO and Fex-Me-IMO samples, in that:
i) according to UV-vis spectroscopy, both Fe-containing samples exhibit UV bands , which can be attributed to ligand-to-metal (O–Fe) charge-transfer transitions of isolated Fe(III) ions in octahedral environment and to a small amount of FexOy nanoclusters [2];
ii) XRD patterns allow calculation of lattice parameter (*a*) values indicating that ionic exchange allows the isomorphic substitution of Al^{3+} by Fe^{3+} without alteration of the lattice parameter.

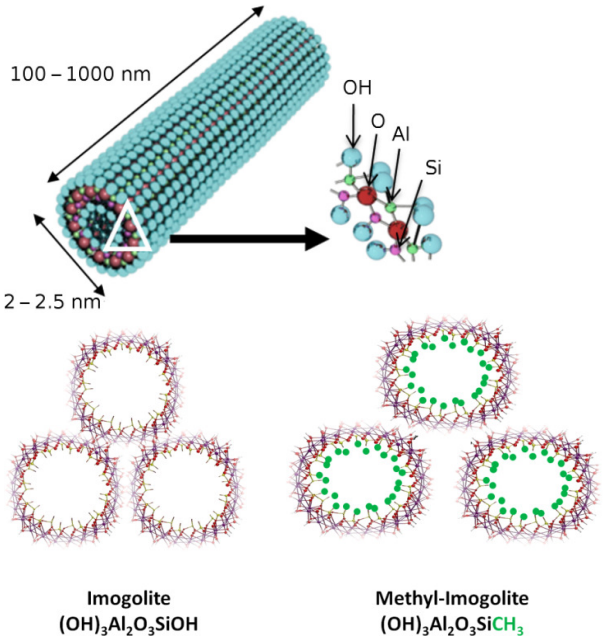

Figure 1: Section of Imogolite and Methyl-Imogolite nanotubes, in which ferric ions can replace Al^{3+}sites [3] , [4].

The ionic exchange therefore is a promising method to allow doping IMO NTs not only with iron, but also with other trivalent cations that could repace external Al, without altering the synthesis medium.

Keywords: Imogolite; nanotubes; isomorphic substitution; Fe-doping; Ion exchanging; adsorption; Direct synthesis.

References:

[1] Shafia, E., PhD thesis., Politecnico di torino.
[2] Wang, Y., Zhang, Q, H., Shishido, T., Takehira, K.,. (2002)., J. Catal., 209, 186-196.
[3] Garrone, E., Ugliengo, P., (1991)., Langmuir., 7, 1409-1412.
[4] Zanzottera, C., Armandi, M., Esposito, S., Bonelli, B., (2012)., J. Phys. Chem., 116, 20417−20425.

*Corresponding author: Prof. Barbara Bonelli
E-mail: barbara.bonelli@polito.it
Tel: +39-3392803713

Nanostructured Polymer Matrix Composites for High Performace Engineering Applications

T. Turcsán,[1,*] L. Mészáros,[1,2]
[1]Budapest University of Technology and Economics, Department of Polymer Engineering, Muegyetem rkp. 3., H-1111 Budapest, Hungary
[2]MTA–BME Research Group for Composite Science and Technology, Muegyetem rkp. 3., H-1111 Budapest, Hungary
*corresponding author, e-mail: turcsan@pt.bme.hu

Abstract: The researchers and developers intend to obtaine favourable mechanical and thermal properties on the field of polymer composites. The thermoset matrix polymer composites have great mechanical properties and relatively good thermal resistance compared to the thermoplastic ones, but they have not as good toughness as the thermoplastic polymer ones, ductile metals and alloys. The high performance polymer composites usually give rigid reactions to the quckly forthcoming and cyclic loads. Rigidity could be caused by the pronouncedly rapid crack propagation and fracture velocity inside of the composite. This is the reason why it is important to improve their toughness without decrease the great mechanical properties (Karger-Kocsis, 2005).
Usually the matrix of the polymer composite is responsible for the toughness of the complete material. Improvement in the toughness of the thermoset resins can be reached by several ways. One of them is creating nanostructure in the material by modificate its morphology. There are several ways to do this modification. On one hand it is possible by giving nanosized additives, nanoparticles to the resin on the other hand there is an opportunity to interblend different type of resins. During the crosslinking process of different mixed resins the compound can be divided to at least two segements by phase separation processes. Because of this phase separation in case of optimal conditions it is possible that nanostructured hybrid resin come into being with co-continuous conformation. In this nanostructured material, there are lots of entanglements of the molecule chains of the componenst by the way they have lots of secondary bounds between them. Additional flexibility and toughness of the matrix material can be reached by this mechanical bounding of named secondary bounds and entanglements. By reason of the mentioned phenomena the crack propagation of the hybrid resin is hampered because of lots of bounds and molecule chain intertanglementsin the material (Turcsán et al, 2014).
Using the mentioned phase separated hybrid resin as matrix material of fibre reinforced composite (Fig 1) it could result improved damping properties by the way enhanced toughness (Mészáros et al, 2014). In case of several fibre reinforcements there is a chance to set their surface threatment that this sizing to result better connenction to one component of the hybrid resin. If the better connected resin to the fibre is less rigid than the other one, it could work in couples with the reinforcement and other resin by the way effect another positive modification for damping properties and toughness.
Another possibly way to modificate the morphological structure of the composite is giving nanoparticles and phase separated nanostructured resin, too.
The main aim of our research work is to create nanostructured high performance fibre reinforced polymer composites for mechanical applications and investigate their morphological and mechanical properties bring into focus the toughness by the way to improve the durability of them.

Keywords: nanostructure, polymer composites, phase separated nanostructure, high performace composites, mechanical applications.

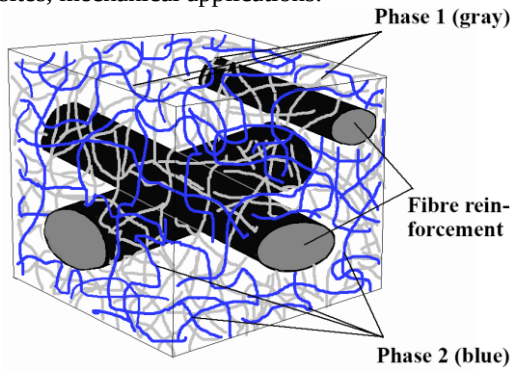

Figure 1: Theoretical structure of the co-continuous nanostructured multiphase system of a hybrid resin matrix fibre reinforced polymer composite

References:

Karger-Kocsis J. (2005) Simultaneous interpenetrating network structured vinylester/epoxy hybrids and their use in composites, in 'Micro- and Nanostructured Multiphase Polymer Blend Systems: Phase Morphology and Interfaces' CRC Press, Boca Raton.

Mészáros L., Turcsán T.(2014), Developemnt and mechanical properties of EP/VE hybrid composite systems, Periodica Plytechnica, Mechanical Engineering, 58, 127-133.

Turcsán T., Mészáros L (2014), Development of high-performance polymer composite with toughened matrix, The Fiber Society Spring 2014 Conference, May 21-23, 2014, Liberec, pp 69-70.

Fatigue properties of basalt fiber and carbon nanotube reinforced hybridcomposites

J. Szakács,[1,*] L. Mészáros [1,2]
[1]Budapest University of Technology and Economics, Department of Polymer Engineering, Muegyetem rkp. 3., H-1111 Budapest, Hungary
[2]MTA–BME Research Group for Composite Science and Technology, Muegyetem rkp. 3., H-1111 Budapest, Hungary
*corresponding author, e-mail: szakacs@pt.bme.hu

Abstract:
More and more researchers think that using an additional third phase might be an effective way to increase the mechanical performance of the polymer composite or endow it with new properties. This third phase can be another matrix component (thermoplastic or thermoset polymer) or reinforcing material. In the first case the main goal is often to create a co-continuous phase system and this way the energy consumption during the fracture process could be increased (Turcsán *et al.*, 2014). In the second case where two different reinforcing materials are used usually the aim is to increase the strength and the stiffness of the material. Beside microfibers as secondary reinforcing materials nanoparticles are also widely used like nanoclays, carbon nanotubes and graphene (Figure 1.).
Carbon based nanoparticles like carbon nanotubes and graphene have unique electrical, thermal and mechanical properties. Moreover graphene has the greatest tensile strength and modulus among the known materials (Lee *et al*, 2008). Nanoparticles have another great property what is the extremely high aspect ratio. The use of this filler can increase the mechanical attribute of the material.
In one of our previous study (Mészáros *et al*, 2013) positive effect of the nanoparticles on the polymers elasticity has been presented. A special cyclic test was carried out where the load was increased in every cycle. It was showed that the graphene and carbon nanotube efficiently decreased the residual deformation of hybrid composites in every load level that resulted in higher rate of elastic recovery compared to matrix material. That mean this material can be used at higher load level with less residual deformation. This statement may mean that this materials have higher life cycle in case of long time loading (creep and fatuigue)

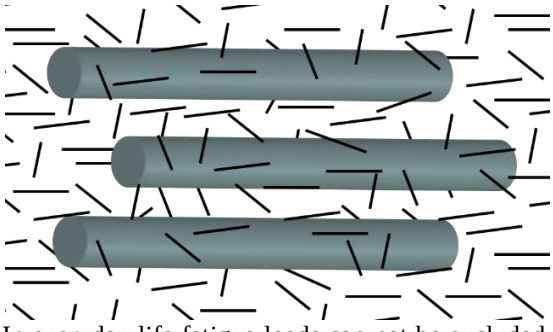

In everyday life fatigue loads can not be excluded in the case of structural polymer composite components. The positive effect of fibre reinforcement on the fatigue properties are well known and deeply investigated. Today, the researchers pay more attention to the fatigue crack propagation and the failure analysis.
The fatigue properties of hybrid reinforced composites is less investigated, however there are some studies that displays the positive effects of the hybridization. Grimmer *et al* (2010) investigated fatigue life of carbon nanotube and glass fibre reinforced epoxy matrix hybrid composites. The presence of relatively low amount of carbon nanotube reduced the cyclic delamination and crack propagation in the material significantly. This effect was more significant at lower levels of cyclic stress.
In this study hybrid composites were produced with carbon nanotube and basalt fibre reinforcement. The goal was to enhance the dispersion of the nanoparticles therefore achieve better quasi-static mechanical and fatigue performance.

Keywords: nanoparticles, carbon nanotube, polyamide, fatigue, hybrid composite

Figure 1: Figure illustrating the base concept of hybrid composites in case of well dispersed nanoparticles (cylinders as fibers and black lines as particles)

References:

Turcsán, T., Mészáros, L. (2014), Development and mechanical properties of carbon fibre reinforced EP/VE hybrid composite systems, *Periodica Polytechnica*, 58, 127-133.

Lee C., Wei X., Kysar J. W., Hone J. (2008), Mesurement of the elastic properties and intrinsic strength of monolayer Graphene, *Science*, 321, 385-388.

Mészáros, L., Szakács, J. (2013), Elastic recovery at graphene reinforced PA 6 nanocomposites. *5th International Nanocon Conference*, Brno, Czech Republic, pp. 1-5. Paper nr. 1955

Grimmer, C. S., Dharan, C. K. H. (2010), Enhancement of delamination fatigue resistance in carbon nanotube reinforced, *Composites Science and Technology*, 70, 901-908.

The influence of redistribution ions in subphase at the properties langmuir monolayer

Chumakov A. S.[1], Ermakov A. V.[1], Kim V. P.[2], Gorbachev I. A.[1], Glukhovskoy E. G.[1]
[1]Departament of nano- and biomedicine technology, Saratov State University named for N.G. Chernyshevsky, Russia
[2]Department of Physics, Moscov State University named for M.V. Lomonosov, Russia

Abstract: Currently, the Langmuir-Blodgett method allows to form monomolecular layers (ML) at the gas-liquid interface and receive a unique layered structure in which each monomolecular layer can have its own chemical composition, crystal structure and orientation of the molecules. Films and Langmuir ML can serve for nanotemplate arranged nanowire arrays, nanotubes or nanoparticles.

The formation of a monolayer and its structure depend on many factors. One of the least studied factors is the influence of the electric field. In this regard, the purpose of this study is to investigate the influence of the direction and magnitude of the electric field on the properties of ML, formed on the surface of water and aqueous solutions of $NiCl_2$.

Our experiments realized for the following cases: in the absence of electric fields, at the different directions of the electric field vector (upwards or downwards), in case of deionized water and $NiCl_2$ aqueous solutions. For these studies we designed the specific electrode system for an existing LB trough and redesigned barriers. The barriers were made in the form of hydrophobic fibers of dielectric material (or wires in the braided PTFE) disposed on the liquid subphase surface. These wires were stretched over a frame, and freely-moving above the upper electrode.

The experiments have revealed: the electric field exerts a significant influence on the formation of monolayers, in particular, during liquid phase formation. The second part of the isotherm (corresponding liquid phase) isotherms were significantly stretched, if subphase of deionized water was used. The increase was about 25% when a voltage to the electrodes was applied. This extension depends not so much on the direction of the vector field, but on the fact that the field is applied. We explain the liquid phase extension by the fact of the charge increasing (and change pH) of the surface region just under the ML. The ions H^+ or OH^- are integrated in the head groups of molecules that leads to the "loosening" of the latter.

If a $NiCl_2$ solution is used as a subphase, then we have the opposite effect. The formation of the liquid phase occurs later under the influence of the field. It is possible that some of the ions OH^- react with Ni^{2+} ions (when a positive potential to the upper electrode is appled) and prevents the salt formation reaction (NiArh), which loosens a monolayer without field. In other polarity tightened ions Cl^-, which do not react with the monolayer because the lower part is charged very negatively, and Ni^{+2} ions move downward, that is blocking the salt formation.
To confirm this assumption we created a new device, which allows us to make a preliminary separation of ions in the water before the experiment, and make a difference in the pH about four units without adding any buffers. This is achieved by using the water-containing vessel, that was divided in 2 parts by a semipermeable membrane (dialysis film) that eliminates the possibility of mechanical agitation of water, but cannot interfere with the free movement of ions. Thus, when we create a difference of potential between the different parts of the vessel, the ions are able to be separated and we obtain virtually pure (from chemical point of view) water, but its acidity will differ from the neutral pH value. Isotherms obtained on the preformed water have more clearly showed effect discovered previously, i.e. the increase of the area of conventional surfactant molecules at the part of liquid phase. This indicates that the separation of ions is a key factor that change the structure of the monolayer when electric field is applied.

Keywords: Langmuir-Blodgett method, monolayers, electric field, pH, isotherms.

The work is supported by grant № 14-12-00275 of Russian Science Foundation and Saratov State University.

References:

Glukhovskoy E.G. (RU), Brezesinski Gerald B. (DE), Gorbachev I.A. (RU), Kim V.P. (RU), Gur'yanov V.A. (RU) Device for the formation of monolayers by the Langmuir-Blodgett method in an electric field // Pat. RU 111297 IPC G01N 13/02. The Patentholder - Saratov State University named after N.G.Chernyshevsky. Published on: 10.12.2011. *Bul. № 34*

Chumakov A., Ermakov A., Kim V., Gorbachev I., Glukhovskoy E. Langmuir monolayers in the electric field // Symposium: Optics & Biophotonics. Saratov Fall Meeting 2013 (SFM'13). 25–28 Sept. 2013. Workshop: Low-dimensional structures III (Oral Report). URL: http://sfm.eventry.org/report/724

Control possibility of separation surfactant from nanoparticles solution by Langmuir method

K.I. Kosolapova [1], A.J.K. Al-Alwani [1], E.G. Glukhovskoy [1,2]
[1]Faculty of Nano- and Biomedical Technologies, Saratov State University, Russia
[2] Department of Educational and Research Institute of Nanostructures and Biosystems, Saratov State University , Russia

Abstract: Nanoparticles rectify it's very difficult due to small size (2-5nm). As well it's difficult due to a small selection of suitable solvents, irreversible adsorption with other materials, aggregation. Aggregation nanoparticles lead to a change in the size of the system elements. Change in the size of the system to make difficult selection of membrane with pore to a certain size.

In this work presented the results of studied that show the possibility of purification by membrane filtration solutions nanoparticles in chloroform/toluene and control possibility of separation undesirable molecules from nanoparticles solution by Langmuir method.

As you know for realization of Langmuir method for studying of monolayer on the water surfaces with very small concentration of solutions of nanoparticles. Typical concentrations are between 10^{-3} and 10^{-4} M.

By the experiment can be realized «inverse-problem» method: the determination of the solution concentration on the base knowledge parameters from compression isotherms.

Present results of experimental use one of the low-cost materials for the membrane. It was used for separation of organic molecules of the stabilizer (oleic acid) from initial solution nanoparticles.

Purification of nanoparticles, stabilized oleic acid, was carried out with using a specially assembled unit for 168 hours. Isotherm compression of the external solution were removing for observation and diffusion control during this time.

The solution of colloidal quantum dots stabilized oleic acid in chloroform to about 10^{-6} M concentration of 500 µl was placed in a dialysis bag which was immersed in the box with chloroform. The internal volume of the solution in the package was 500 µl , the volume of the external solution in a bank – 50 ml.

As a vessel for carry through a membrane filter was taken jar reagent plastic screw cap 100 ml.

Control and monitoring the diffusion of the surfactant through the membrane was done by measuring the surface pressure (isothermal compression) of the external solution. To measure the surface pressure setting used KSV Nima LB Trough KN2002.

Compression isotherms were recorded every 24 hours. For cleanliness before each measurement surface degreasing bath and purified with chloroform. As subphase used deionized water with a resistivity of 18 MOhm × cm. On the surface of the water each time make the same amount of material from the outer volume (of the solution in a glass container) – 500 µl. (Fig.1)

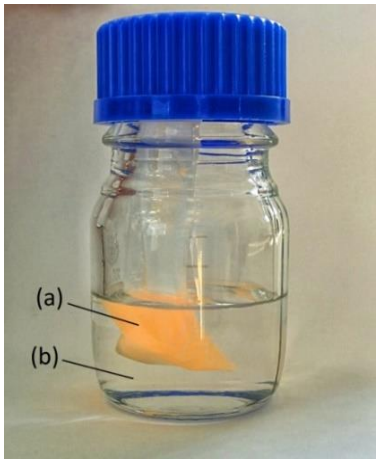

Fig.1. The process of separation: nanoparticles membrane solution bag (a), chloroform (b).

To investigate the changes in the number of surfactant in the external volume of the solution used Langmuir-Blodgett technique. In the process of compression isotherms were taken the outside solution during the membrane filtration of the solution of nanoparticles.

It is noticeable that the increases of maximum surface pressure with increasing filtration time. Obviously the Reducing of length of gas phase of external solution is due to increase the number of unbound molecules in the external volume of the solution. This growth is due to the process of diffusion of unbound molecules of oleic acid through polyethylene membrane.

Keywords: separation, purification, nanoparticles, pressure isotherms, Langmuir monolayer, Langmuir–Blodgett technique.

The work is supported by grant № 14-12-00275 of Russian Science Foundation and Saratov State University.

Analyzing size dependence of thermal conductivity of suspended graphene with Null-Point Scanning Thermal Microscopy

Gwangseok Hwang,[1,2] Ohmyoung Kwon,[1,*]
[1]School of Mechanical engineering, Korea University, Seoul, Republic of Korea
[2]TSP Nanoscopy, Seoul, Republic of Korea

Abstract: The characteristic length of graphene devices is approaching or even getting shorter than the mean free path of phonon. Thus, the size effect on the thermal conductivity of graphene should be seriously considered in the development of graphene-based nano-devices. However, current techniques used to measure the thermal conductivity of graphene, such as Raman spectroscopy and the thermal bridge method, are not suitable for observing such a size effect at the sub-micron scale. In this study, we rigorously re-derived the principal equation of null point scanning thermal microscopy (NP SThM) in terms of measuring the thermal properties to explain how this technique, which has already been proven to resolve the major problems of conventional SThM and be able to quantitatively measure the temperature profile (Hwang *et al.*, 2014; Yoon *et al.*, 2014), can be effectively utilized for quantitatively measuring the local thermal resistance with a nanoscale spatial resolution. Using NP SThM, we measured the relative change in the thermal conductivity of suspended chemical vapor deposition (CVD)-grown graphene disks with radii of 50–3680 nm and estimated the absolute value of the thermal conductivity of these disks in a diffusive regime (Figure 1, 2). We performed a theoretical analysis to demonstrate that the relative changes and absolute values of the thermal conductivity of the graphene disks were consistent. As demonstrated in this study, NP SThM will be very useful for the quantitative thermal characterization of not only CVD-grown graphene but various other nano-materials and -devices.

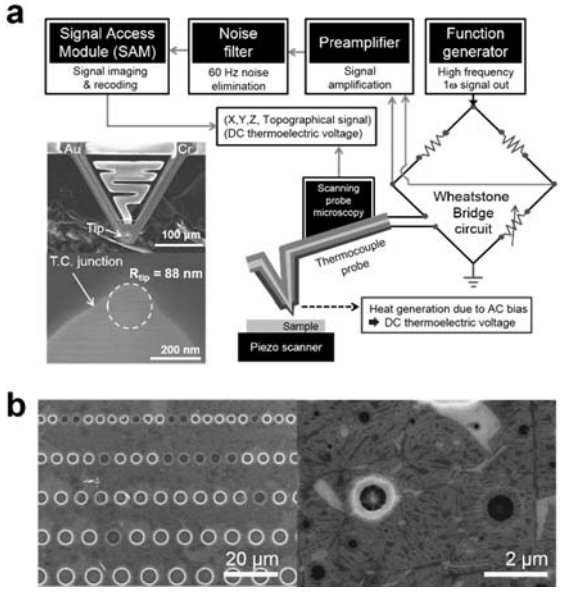

Figure 1: (a) Schematic diagram of experimental setup for NP SThM and SEM images of thermocouple SThM probes. (b) SEM images of micro- and nano-scale suspended CVD-grown graphene disks.

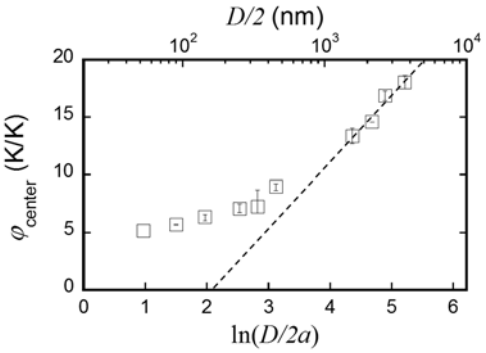

Figure 2: Value of φ at center of disk (φ_{center}) measured by NP SThM as function of ln (D/2a) for ten suspended graphene disks with radii of 50–3680 nm. Because $\varphi_{center} = (R_s + R_c)/R_p$ and R_p and R_c remain constant during the scanning, a change in φ_{center} means a change in R_s.

Keywords: graphene, thermal conductivity, null point scanning thermal microscopy (NP SThM), ballistic heat transport, diffusive transport, size effect, SThM probe, nanoscale thermal measurement.

Acknowledgments:
This work was supported by the Basic Science Research Program (NRF-2013R1A1A2012138) and Nano-material Technology Development Program (Green Nano Technology Development Program) (No. 2011-0030146) through the National Research Foundation of Korea (NRF) funded by the Ministry of Education, Science and Technology.

References:

Hwang, G., Chung, J., Kwon, O. (2014) Enabling low-noise null-point scanning thermal microscopy by the optimization of scanning thermal microscope probe through a rigorous theory of quantitative measurement, *Rev. Sci. Instrum.*, 85, 114901.

Yoon, K., Hwang, G., Chung, J., Kim, H., Kwon, O., Kihm, K. D., Lee, J. S. (2014) Measuring the thermal conductivity of residue-free suspended graphene bridge using null point scanning thermal microscopy, *Carbon*, 76, 77-83.

Three-Arm Star Block-Copolymers: Enzyme-Inspired Catalysts for Oxidation of Alcohols in Water

C. Mugemana, B.-T. Chen, K. V. Bukhryakov and V. Rodionov*[1]
[1]KAUST Catalysis Center and Division of Physical Sciences and Engineering,
King Abdullah University of Science and Technology, Thuwal, 23955-6900,
Kingdom of Saudi Arabia
*Email: valentin.rodionov@kaust.edu.sa

Abstract: The oxidation of alcohols to aldehydes has become the most challenging class of oxidation reaction in organic chemical synthesis since the large-scale applications are limited by safety issues associated with the combination of O_2 and organic solvents. The Cu/TEMPO (2,2,6,6-tetramethyl-1-piperidine-N-oxyl) system has emerged as one of the most attractive catalysts for selective aerobic oxidation of primary alcohols. (Stahl et al., 2011) The established protocols for Cu/TEMPO catalyzed alcohol oxidation strongly favor organic solvents, especially acetonitrile. We aimed to design an enzyme-inspired functional macromolecular architecture that could enable the transfer of this catalytic system to pure water. Such a transfer could enable large-scale applications of Cu/TEMPO, while circumventing the usual safety concerns associated with combining oxygen and organic solvents

The use of dendrimers (Astruc et al, 2001) and hyperbanched polymers (Fréchet et al, 2005) has been a successful strategy for improving catalyst dispersion properties and creating optimal local solvent environment. In this study, we present a pathway to enzyme-inspired catalytic materials based on star block-copolymers with limited branching. (Rodionov et al, 2014) These polymers incorporate hydrophilic, superhydrophobic, and polydentate metal-binding characteristics. (Figure 1) Starting with a tripodal, TBTA – inspired NMP initiator, a library of flurous amphiphilic star block copolymers was synthesized. These polymers assembled into well-defined nanostructures in water, and their mode of assembly could be controlled by changing the composition of the polymer. The prepared micelles were used for enzyme-inspired catalysis of alcohol oxidation.

Keywords: star polymers, enzyme-inspired catalyst, micelles, vesicles, homogenous catalysis, alcohol oxidation, block coppolymer self-assembly.

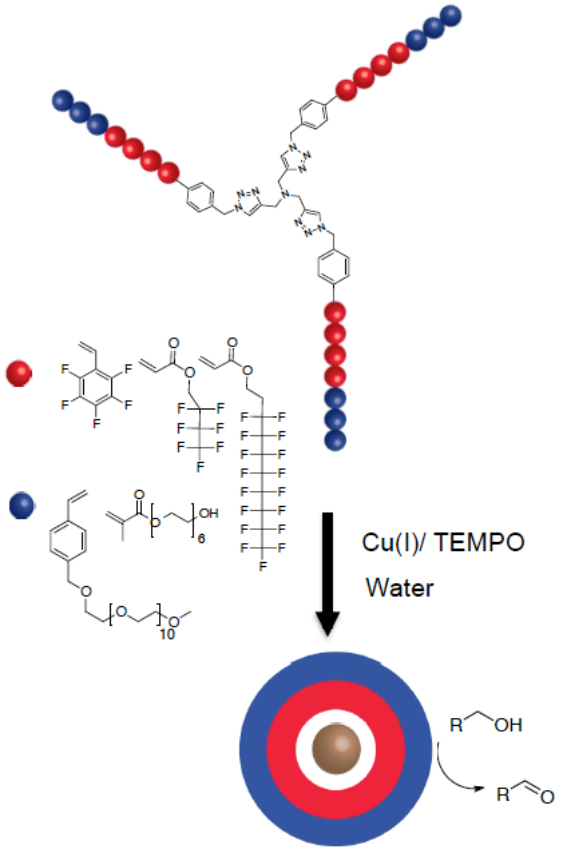

Figure 1: Representative scheme of three-arm block copolymers, their self-assembly in water and catalytic aerobic alcohol oxidation.

References:

Hoover, J.M., Stahl, S.S., (2011) Highly Practical Copper(I)/TEMPO Catalyst System for Chemoselective Aerobic Oxidation of Primary Alcohols *J. Am. Chem. Soc.* 133, 16901-16910.

Astruc, D., Chardac, F. (2001), Dendritic catalysts and dendrimers in catalysis, *Chem. Rev*, 101, 2991-3024

Helms, B., Guillaudeu, S.J., Xie, Y., Mcmurdo, M. Hawker, C.J., Fréchet, J.M.J. (2005), One-pot reaction cascade using star polymers with core-confined catalyst, *Angew. Chem. Int. Ed.*, 44, 6384-6387.

Mugemana, C., Batian, C.-T., Bukhriakov, K.V. Rodionov, V. (2014) Star Block-Copolymers: Enzyme-Inspired Catalysts for Oxidation of Alcohols in Water, *Chem. Commun.* 50, 7862-7865.

Hydrophobic Material with Polymeric Shell

G. Sugurbekova, A.Seralin, G.Demeuova, M.Baisariyev
Nazarbayev University, National Laboratory Astana, Astana city, Kazakhstan

Abstract:
Development of new materials and modification of surface, physical and chemical properties of nanostructured objects can greatly expand the range of possibilities for high technology and brings to the new level their application in various industries.

This study aims to obtain hydrophobic materials for multipurpose applications, including moisture-saving technologies in agriculture and construction.

We have proposed technology of producing superhydrophobic materials based on polymer, sand and fertilizer, which allows to regulate hydrophobic properties of materials by directional formation and surface modification. Superhydrophobic materials produced using this cheap and environmentally friendly technology exhibit high thermal stability and good performance. Use of complex mineral fertilizers of prolonged action also promotes the formation of superhydrophobic structured material.

Surfaces of superhydrophobic powder have complicated relief. Air bubbles can stabilize on the rough surface of the material, as a result forming a stable "air bag" condition in the cavities of the relief. When tested with water for water resistance, fluid was observed to partially flow over the gas phase than solid surface. At the liquid-gas interface, friction is very limited, which leads to a sudden increase of sliding capacity of such surfaces.

Studies were conducted to determine the wetting contact angle using a goniometer to determine the degree of hydrophobicity. Several types of superhydrophobic powders were obtained with contact angles of about 157 ° (Figure 1). Scanning electron microscopy (SEM) images depicting microstructure of the surface of materials showed that the composite materials consist of microparticles with core-shell structure.

The composition of the structures was studied using FTIR-spectral analysis method. IR spectra (Figure 2) of initial, intermediate and final products shows an acute, intense peak at 1258 cm^{-1}, indicating the presence of valence vibrations of $\vartheta_{(Si\text{-}CH3)}$. Relatively low peak at 2355 cm^{-1} refers to the fluctuations of hydrocarbon group CH_2, whereas bands at 2960 cm^{-1} refers to the fluctuations of CH_3. In the region from 787 to 790 cm^{-1} there is a very intense band with a shoulder at 668 cm^{-1}, which is also an indication of Si-C bonding. In the area of 1040 cm^{-1} Si-O-Si bridging is identified, followed by Si-O at 1010 cm^{-1}.
Keywords: Hydrophobic powder, hydrophobization, core-shell structure

Figure 1: Water droplet at the surface of hydrophobic material with a contact angle of 157°.

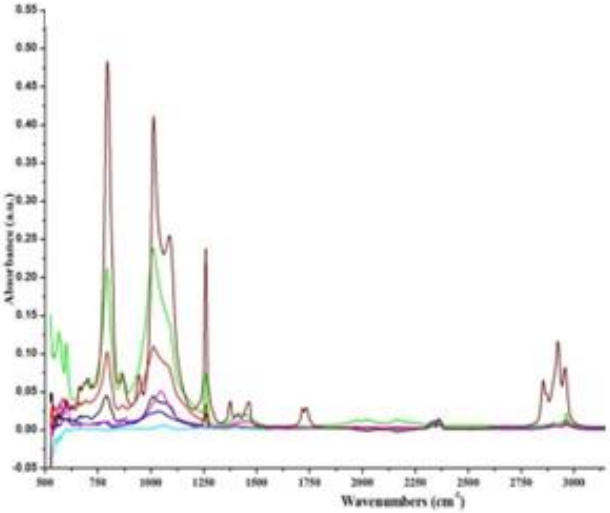

Figure 2: IR spectra of initial, intermediate and final products

Acknowledgement

This project was funded by Office of commercialization of PI "Nazarbayev University Research and Innovation System" based on Nazarbayev University.

New Performances of Fluorescent Photosensitive Glass Ceramics for Petabyte Optical Disk 3D Written by Direct Laser Interaction

S. I. Jinga,[1,*]E. Pavel[2]
[1*]Faculty of Applied Chemistry and Materials Science, "Politehnica" University of Bucharest, 011061 Bucharest, Romania
[2]Storex Technologies, 020892 Bucharest, Romania

Abstract: We report novel results for 3D recording of an optical disk with ultra-high density by changing glass matrix compositions and equilibrium between silver nanocrystals and fluorescent nanostructures. In the same time we try to find out which are the best ways to minimize the distances between fluorescent structures in 3D architectures of optical disks and to increase fluorescence intensity of 5nm cylindrical structure in order to achieve good performances in reading process of 3 D optical disk.
Our previous results [1-3] demonstrate the possibility to exceed the diffraction limit in glass- ceramics using a laser radiation with low energy.
Also, we demonstrate the performance of glass – ceramics which is able to storage up to density greater than 6 PB/disk [4].

Keywords: fluorescent photosensitive glass-ceramics, 3D direct laser writing, optical disk, data storage.

References:

1. Pavel E, Mihailecu M, Nicolae V B, Jinga S, Andronescu E, Rotiu E, et al. Holographic testing of fluorescent photosensitive glass-ceramics. Opt Commun 2011;284:930–3.

2. Pavel E, Jinga S, Andronescu E, Vasile B S ,Rotiu E ,Ionescu L, et al. 5nm structures produced by direct laser writing. Nanotechnology 2011; 22:025301.

3. Pavel E, Jinga S, Andronescu E, Vasile B S, Kada G, Tosa N,et al. 2nm quantum optical lithography. Opt Commun 2013; 291:259–63.

4. Pavel E, Jinga SI, Vasile BS, Dinescu A, Marinescu V, Trusca R, et al. Quantum optical lithographyfrom 1nm resolution to patterntransfer on silicon wafer. Opt LaserTechnol, 2014; 60:80–4

Pavel E, Jinga SI, Vasile BS, Dinescu A, Tosa N, Trusca R, 3D direct laser writing of Petabyte Optical Disk, Opt LaserTechnol, 2015; 71, 45-49

Iron Nanoparticles-Doped Water Treatment Residues for Arsenic Removal from Industrail Wastewater

P. Sarntanayoot, A. Imyim*
Department of Chemistry, Faculty of Science, Chulalongkorn University, Bangkok 10330, Thailand

Abstract: Arsenic (As) has been used in various industrial fields including agriculture, electronics, and metallurgy. Industrail wastewater can be contaminated by high levei of arsenic. Therefore, methods for the removal of arsenic from contaminated wastewater are critical and necessary. Adsorption is a commonly employed method for arsenic removal from aquous media. Various types of adsorbent have been developed. Arsenic is mostly found in inorganic forms which are trivalent (arsenite or As(III)) and pentavalent (arsenate or As(V)). Most of th adsorbents are effective only for As(V) removal. As(III) has to be oxdised using oxidizing agents such as chlorine dioxide, hypochlorite, potassium permanganate and monochloramine (Sorlini and Gialdini, 2012) to As(V) before its removal by adsorption. Zero-valent iron nanoparticles were also employed for simultaneous oxidation and reduction of As(III) to promote its removal efficiency (Du *et al*., 2013, Ramos *et al*., 2009, Yan *et al*., 2012). Low cost adsorbents such as water treatment residues (WTR) showed arsenic removal potential towards As(III) and As(V) due to alum and ferric hydroxide composition in the WTR (Kim *et al*. 2012). However, the removal efficiency of As(III) was still low. Thus in this research, the WTR is doped by iron nanoparticles and used for the removal of arsenic. The amount of iron was varied in the range of 2-10 %(w/w). The maximum As(III) adsorption capacities were 9.4, 11.8, 13.2,13.5, 15.1, 24.2 mg/g for 2, 4, 5, 6, 8, and 10 %(w/w) of loading iron. While the maximum As(III) adsorption capacity of bare WTR was 2.3 mg/g. The result reveals that iron nanoparticles plays an important role in the enhancement of adsorption capacity of As(III). In addition, the maximum As(V) adsorption capacity was 32.0 mg/g for 10 %(w/w) of loading iron. The pictures of adsorbents as well as SEM image were shown in Figure 1. The prepared materials shows a promising applicability for arsenic removal form high arsenic-contaminated industrail wastewaters.

Keywords: iron nanoparticles, water treatment residues, arsenite, oxidation-adsorption, removal, wastewater.

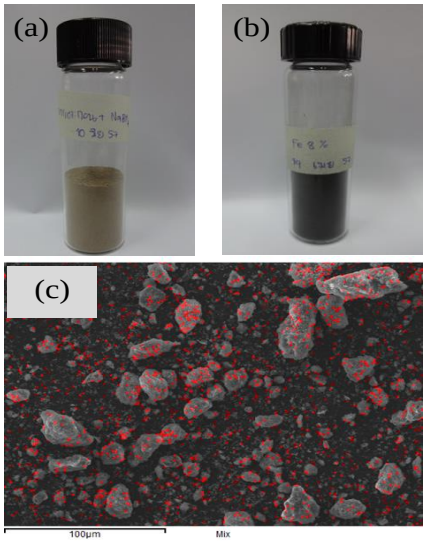

Figure 1: Photographs of (a) water treatment residues, (b) iron nanoparticles-doped water treatment residues, and (c) SEM image with EDX mapping of Fe (red spots).

References:

Du, Q., Zhang, S., Pan, B., Lv, L., Zhang, W., Zhang, Q. (2013) Bifunctional resin-ZVI composites for effective removal of arsenite through simultaneous adsorption and oxidation, *Water Res.*, 47, 6064-6074.

Kim, Y.S., Kim, D.H., Yang, J.S., Baek, K. (2012) Adsorption characteristics of As(III) and As(V) on alum sludge from water purification facilities, *Sep. Sci. Technol*., 47(14-15), 2211-2217.

Ramos, M.A.V., Yan, W., Li, X., Koel, B.E. (2009) Simultaneous oxidation and reduction of arsenic by zero-valent iron nanoparticles: Understanding the significance of core-shell structure, *J. Phys. Chem. C.*, 113, 14591-14594.

Sorlini, S., Gialdini, F. (2012) Conventional oxidation treatments for the removal of arsenic with chlorine dioxide, hypochlorite, potassium permanganate and monochloramine, *Water Res.*, 44, 5653-5659.

Yan, W., Lien, H.L., Koel, B.E., Zhang, W.X. (2012) Critical review iron nanoparticles for environmental clean-up: Recent developments and future outlook, *Environ. Sci.: Processes Impacts.*, 15, 63-77.

Transfer and biotransformation of gold and silver nanoparticles through aquatic food chain

Xingchen Zhao, Qunfang Zhou, Guibin Jiang
State Key Laboratory of Environmental Chemistry and Ecotoxicology, Research Center for Eco-Environmental Sciences,Chinese Academy of Sciences, Beijing 100085, PR China

Abstract: Considerable attention has been paid recently to nanomaterials not only because of their application possibilities but the potential toxicities to humans and ecosystems. As an emerging environmental pollutant with unknown eco-environmental risks, nanomaterials should not relax our vigilance. Some nanomaterials process similar properties as persistent toxic substances (PTSs) such as less biodegradable and lipophilic. Pollutants like mercury, dichlorodiphenyltrichloroethane, hexachlorocyclohexane have taught us enough lessons how they display destructive forces to the environment (Chikuni *et al.*, 1997; Qiu *et al.*, 2005; Phillips *et al.*, 2005). The risk of nanoparticles entering these environments, as well as the effects on human health from people having contact with the nanoparticles, needs to be carefully assessed and investigated. Among all the food chains, fish-crustacean is one of the pillars of the global aquatic ecosystem. Besides, fish is an economically important species that have long been consumed by humans. Trophic accumulations of nanomaterials from the preys to fish give rise to the possibility that they may transfer finally to humans. In this study, we investigated the trophic transfer of noble metal nanoparticles from fairy shrimp (*Eubranchipus vernalis*) to Japanese medaka (*Oryzias latipes*). Four kinds of nanoparticles, hexadecyltrimethylammonium bromide (CTAB) coated silver nanospheres (CSNSs), CTAB coated gold nanospheres (CGNSs), CTAB coated gold nanorods (CGNRs), and poly(sodium-p-styrenesulfonate) coated gold nanorods (PGNRs) were employed to study the effects of shape, surface coating and core in the trophic transfer. Our findings hold the promise to highlight the potential for trophic transfer as an ecological impact of nanomaterials.

Keywords: silver nanoparticle, gold nanoparticle, uptake and depuration, bioaccumulation, biomagnification, biotransformation, food chain.

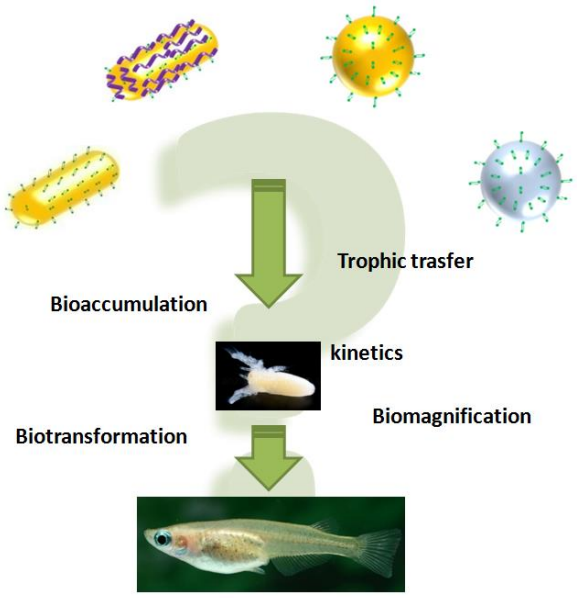

Figure 1: Figure illustrating the questions that we are tempting to solve experimentally: For the four kinds of materials, which one is likely to biomagnify? Which are the target organs for higher trophic level animals and what are the resulting effects for these organs after accumulation? Will nanoparticles transform chemically and physically as they travel up through food chains?

References:

Chikuni, O., Nhachi, C.F., Nyazema, N.Z., Polder, A., Nafstad, I., Skaare J.U. (1997) Assessment of environmental pollution by PCBs, DDT and its metabolites using human milk of mothers in Zimbabwe, *Sci. Total Environ.*, 1-2, 183-190.

Qiu, X., Zhu, T., Yao, B., Hu, J., Hu, S. (2005), Contribution of dicofol to the current DDT pollution in China, *Environ. Sci. Technol..*, 12, 4385-4390.

Phillips T.M., Seech A.G., Lee H., Trevors J.T. (2005), Biodegradation of hexachlorocyclohexane (HCH) by microorganisms, *Biodegradation*, 4, 363-392.

Nanotechnology in Food Packaging Industry: Opportunities and Challenges

Vasco Teixeira
GRF-Functional Coatings Group, Physics Department, University of Minho
PT-4800-058 Guimaraes, Portugal
Tel: +351-253510465/00, Fax: +351-253510401, Email: vasco@fisica.uminho.pt

Abstract: Nanosciences and nanotechnologies are highly promising areas for research and industrial innovation, with a potential both to boost the competitiveness of many industries which will lead to new emerging and fast growing markets. It is predicted that nanotechnology production approaches will change about 25% of the food packaging business in the next decade, which means a yearly over $ 30 billion market. The major market trends include enhancing the performance of packaging materials, prolonging shelf life, antimicrobial packaging and interactive/sensorial packaging.

One of the main priorities in food packaging technology is to keep the original properties of the food. This goal is achieved by keeping all the nutrients in the original conditions, by ensure minimum interaction between environment and the packaged food and reducing microbial growth

In the field of nanoparticles and nanotechnology-based thin films, new approaches using nanoscale effects can be used to design, create or model nanocomposite systems with significantly optimized or enhanced properties of high interest to the food, health and biomedical industry. With the development of nanotechnology in various areas of materials science the potential use of novel surfaces and more reliable materials by employing nanomaterials and nanostructured thin films in food packaging, security pharmaceutical labels, novel polymeric containers for food contact, medical surface instruments, bio-implants, and even coated nanoparticles for bionanotechnology can be considered.

The use of plastic containers in the food and beverage market has dramatically increased because they are lightweight, unbreakable, convenient, resealable and they may be clear. PET bottles have gradually replaced glass bottles and metal cans as the most common packaging for liquid foods, such as carbonated soft drinks, tea, water, soy sauce and edible oil.In this field of new packaging technologies, nanostructured architectures coatings such as nanocomposite films are given the unique role of enhancing food impact over the consumer's health. For example, the unique properties of diamond like carbon (DLC) film, including its chemical inertness and impermeability, make it possible for new applications in food, beverage and medical market segments. The ability of using thin films and nanoparticles with transparent properties a more flexible and transparent packaging materials will provide the consumers with fresher and customized packs where the products can be observed as they are.

In this presentation it will be presented an overview of the nanotechnology approaches to produce nanostructured materials for food and health industry. Topics to be discussed include introduction to nanocoatings concepts (from functional nanocomposite and graded coatings to smart nanomaterial surfaces used in packaging and biomedical industry) produced by clean PVD technologies (Physical Vapour Deposition) and other deposition techniques. An overview of the current research, existing technological applications and future industrial materials and components will be highlighted. As example for future trends in nanotech-based food packaging will also include research and development on sensorial packaging which can monitor the food and transmit information on its quality. For instance, the ultimate pH of meat greatly affects its quality. Monitoring this parameter can give to consumers information regarding manner of transportation of animals from the farm to the abattoir; diet restrictions; mixing animals of different lots and pathological conditions. With embedded nanosensors in the packaging surface materials, consumers will be able to check the food quality inside or even to track the history of the pack. Electronics built on thin film substrates could be used in future sensory packaging applications (examples include nanoRFIDs).

Inkjet printed polymer functionalized CNT gas sensor with enhanced sensing properties

A. S. Alshammari[1,2], M. R. Alenezi[2,3], K. T. Lai[2] and S. R. P. Silva[2]
[1]Department of Physics, College of Science, University of Hail, P.O. Box 2440, Hail, Saudi Arabia
[2]Advanced Technology Institute, Faculty of Engineering and Physical Sciences, University of Surrey, Guildford, GU2 7XH, UK
[3]College of Technological Studies, PAAET, P.O. Box 42325 Shuwaikh, Kuwait

Abstract: Gas sensing devices receive a considerable interest and can be found in wide range of domestic and industrial applications[1,2]. Here we report on fully printed carbon nanotubes gas sensors on flexible substrate with improved ethanol sensing characteristics. The sensors were fabricated via two simple steps: printing of the electrodes and the sensor active layer. The nanotubes were functionalised with carboxylic acid, surfactant and PEDOT:PSS and their sensing performance is investigated. The performance analysis shows significant enhancement in the sensitivity of the sensor with polymer wrapped nanotubes in comparison with other functionalisation methods with enhancement factor greater than 2.5. Moreover, a remarkable improvement in the response and recovery time of the sensor after polymer functionalisation is noticed. The combination of inkjet printing technique and polymer functionalised nanotubes could pave the way towards flexible, solution processable, low cost and high performance gas sensors.

Keywords: carbon nanotubes, polymer functionalization, inkjet printing, gas sensor.

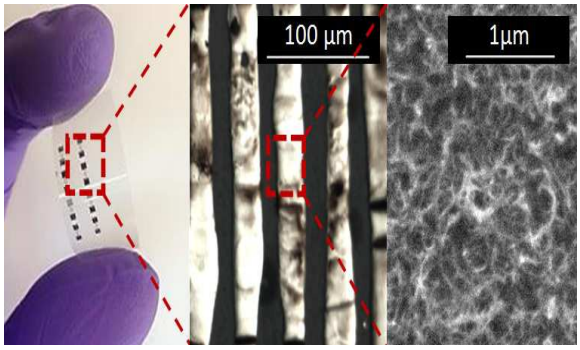

Figure 1: Figure shows a photograph of the printed gas sensor (left), optical microscope image of the printed silver interdigitated electrodes (middle) and SEM image of the printed carbon nanotubes (right).

References:

[1] Liu, C.-K., J.-M. Wu, and H.C. Shih, Sensors and Actuators B-Chemical, **150(2)** (2010) p. 641-648.

[2] M.F. Mabrook, C. Pearson, A.S. Jombert, D.A. Zeze, M.C. Petty, Carbon, **47(3) (**2009) p. 752-757.

Nanoindentation and image characterization of apple tissue and isolated cells (*Malus domestica*) by means of atomic force microscope

Cárdenas-Pérez, S.[1], Chanona-Pérez, J.[1], Neri-Torres, E.E., Marín-Bustamante, M.Q.[1], Cásarez-Santiago, R.G. [1] Méndez-Méndez, J.V.[2], Calderón-Domínguez, G.[1], Suárez-Najera E.[1]

[1]Escuela Nacional de Ciencias Biológicas-Instituto Politécnico Nacional. Prolongación de Carpio y Plan de Ayala s/n México D.F., C.P.11340. [2]Centro de Nanociencias y Micro y Nanotecnologías- Instituto Politécnico Nacional. Luis Enrique Erro s/n, Zacatenco, México

Abstract: The climacteric fruits undergo many morphometric changes during its storage and processing. Therefore, a method to evaluate the cell elastic properties is needed to explain the behavior of fruits during handling and food processing after harvesting at a micro and nanoscale. For this purpose, in this work it is proposed to indent tissue and isolated cells of apple (Golden delicious) using an atomic force microscope (AFM, Bruker, Bioscope Catalyst ScanAsyst, USA) with an indenter probe (NP-10/Sanasyst, Bruker, USA) was proved in order to obtain the corresponding force curves and Young's modulus (YM). The YM is an important parameter of stiffness already reported in literature as an important mechanical property of biologic samples (Milani et al. 2011). The benefit of the AFM is that it has the possibility to combine nano-mechanical properties with topography imaging, which could be very useful for the study of structure-related mechanical properties of fruits at the sub-cellular scale. The isolation of fruit cells in the apple was developed by a simple isolation technique (McAtee et al. 2009) and the tissue was obtained by using a bi-shave which allows to obtain thin slices of apple. Once the cells were isolated and thin tissue were also obtained, the respectively structure was observed in a light microscope for its morphological characterization (Nikon Eclipse Ni , Japan) which is adapted with a digital sight system (Nikon, DS-L3, Japan) this allows the capture of cell images in RGB color. These were analyzed with the software ImageJ v. 1.47 (National Institutes Health, Bethesda, MD, USA) and the shape of cells was characterized (diameter and circularity). The nanoindentation was carried out with the AFM in tissue cells as well as in isolated cells and it was obtained its respective force curves by using the Nanoscope analysis v1.4 software (Bruker, USA) from which the YM was determined by fitting each curve with Hertz model. In Figure 1a and 1b it is shown a the corresponding height image with a regular matrix (8 x 8 points) of nanoindentation points in apple tissue and isolated cell respectively, from which it is obtained the individual force curves as shown in Figure 1c. The force curve is formed by an initial curve (approaching curve) and a second curve (retraction curve) from which it is adjusted the Hertz model in order to obtain YM. The characterization of the isolated cells in 250 total samples showed a slighter difference in cell diameter with 210 ± 27 μm and circularity of 0.68 against cells in tissue with a diameter of 201.91 ± 42 μm and a circularity of 0.53. Otherwise, the YM was obtained in 10 different areas of 5 μm from tissue and isolated cell and a total of 640 curves were obtained. The YM average obtained was 0.740 ± 0.59 MPa for nanoindentation in tissue and 0.274 ± 0.16 MPa in isolated cells, these values correspond to some YM already obtained in other studies (Zdunek and Kurenda 2013). In overall, these studies are particularly useful in fruits because they could help us to explain the mechanical behavior that exists at nanometric level as well as the key of the mechanical changes that occur during post-harvest.

Keywords: nanoindentation, AFM, young´s modulus

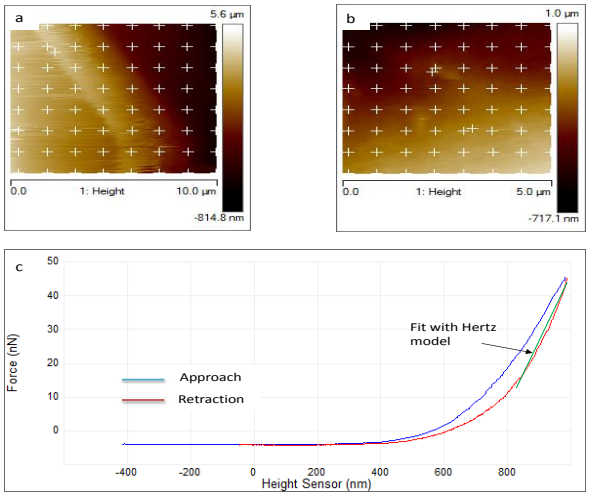

Figure 1 a and b. Illustrates the typical matrix of nanoindentation points from which it is generated the force curves in apple tissue and isolated cell respectively. c. Typical force curve obtained from the NanoScope Analysis software and fitted with Hertz model.

References:

Milani, P., Gholamirad, M., Traas, J., Arnéodo, A., Boudaoud, A., Argoul, F., Hamant, O. (2011). In vivo analysis of local wall stiffness at the shoot apical meristem in Arabidopsis using atomic force microscopy. Plant J 67: 1116–1123.

McAtee, P. A., Hallett, I. H., Johnston J.W., and Robert J. S. (2009). A rapid method of fruit cell isolation for cell size and shape measurements. Plant Methods. 5:5 46-48.

Zdunek, A., Kurenda, A. (2013). Probing plant cell mechanical properties with the atomic force microscope. InsideFood Symposium, 9-12 April 2013, Leuven, Belgium.

The role of the glycocalyx in cellular interactions between lung carcinoma cells and the endothelium

Katarzyna Malek-Zietek, Marta Targosz-Korecka, and Marek Szymonski
Center for Nanometer-Scale Science and Advanced Materials, NANOSAM, Faculty of Physics, Astronomy, and Applied Computer Science, Jagiellonian University, Krakow, Poland

Abstract:

A detailed understanding of the tumor extravasation mechanism is crucial for designing any therapeutic treatment against circulating tumor cells (CTCs) in the bloodstream. The endothelial glycocalyx (eGC) is an intravascular sugar-rich compartment that facilitates gliding of cells in the vascular network, particularly the CTCs. For several pathophysiological states of endothelial cells (ECs), such as inflammatory processes, eGC collapses, gradually shrinks and drops its negative charge. Under such conditions permeability of CTCs trough endothelium is higher and creation of metastases is much more likely. Adhesive interactions between cancer cells and the endothelium strongly depend on the structure of the glycocalyx. Therefore, we characterized the eGC of Primary Pulmonary Artery Endothelial Cells (PHAEC) and the glycocalyx layer of lung carcinoma cells (A549) cultured on fibronectin-rich surface. Nanoindentation spectroscopy with a spherical AFM probe was used to determine the eGC thickness and eGC stiffness before (reference) and after treatment of cells with heparinase I, heparin. Later, the adhesive interactions between lung cancer cells and ECs have been studied. A novel approach was employed to attach the living interactions were validated for living cells containing either a native, or enzymatically digested glycocalyx. Multiparameter analysis of the measured force-distance curves demonstrated that reduction of the glycocalyx layer by heparinise I caused stronger adhesive interactions between A549 cells and PHAEC. Adding to the measurement system heparin instead of heparinase I caused renewal of the glycocalyx and decrease of adhesive interactions between cells. Therefore, we conclude that the structure of the eGC strongly affects the adhesion process between CTCs and the endothelium.

Keywords: glycocalyx, endothelial cells, cancer cells, metastasis, nanoindentation spectroscopy, AFM-based single cell force spectroscopy.

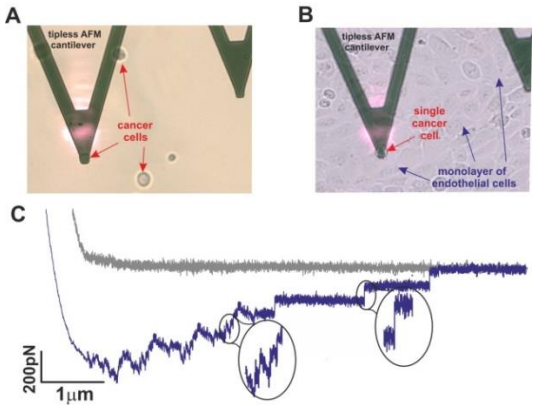

Figure 1: Methodology of single-cell force spectroscopy. **A)** Attaching a living cancer cell to the tip-less AFM cantilever. **B)** Monitoring adhesive interactions between cancer cell and ECs. **C)** Example of the force-distance curve.

Changes of the endothelium nano-mechanics in response to the vascular dysfunction – ex vivo studies for murine model of diabetes

Magdalena Jaglarz[1], Katarzyna Malek-Zietek [1],Marta Targosz-Korecka[1] ,
Stefan Chlopicki[2] and Marek Szymonski[1]
[1]Center for Nanometer-scale Science and Advanced Materials, Department of Physics of Nanostructures and Nanotechnology, Institute of Physics, Jagiellonian University, Prof. Stanislawa Lojasiewicza 11, 30-348 Krakow, Poland
[2] Jagiellonian Centre for Experimental Therapeutics (JCET), Bobrzynskiego 14, 30-348 Krakow, Poland

Abstract:
Endothelium plays an essential role in regulating blood pressure and vascular homeostasis.
The main purpose of the presented study was to relate the observations performed *in vitro* to classical *ex vivo* and *in vivo* models of endothelial dysfunction. Characterization of the endothelial nano-mechanics was performed for the non-fixed aorta in a murine model of hypertension induced by N-nitro-L-arginine methyl ester (L-NAME) as well as in diabetes model (db/db mice).
We have conducted analysis of changes in the morphology and elasticity of the first (from the lumen side) layer (endothelium + basal lamina) of the mouse aorta in healthy and pathological tissues. Elastic properties (stiffness) of the inner tissue surface were characterized using nanoindentation spectroscopy with a colloidal AFM tip, for various areas of the aortic wall.
Both models used in our studies are associated with the development of endothelium dysfunction, which affects the ability to contraction/diastole of the entire vessel. Additionally, biochemical analysis was used in order to determine NO production wich is correlated to nano-mechanical properieties.
Based on AFM nanoindentation model, the stiffnes parameters were determined for various stages of the diabetes development.The nanoindentation measurements revealed changes in stiffnes prameter of the first layer prior to NO release.The qualitative analysis of the tissue elasticity indicates that the above-mentioned diseases induce nanomechanical changes in the first layer of the aorta.

Keywords: Atomic Force Microscopy, Hyperglycemia, hypertension , vascular dysfunction.

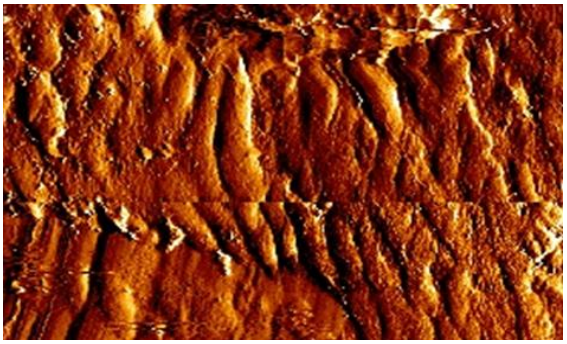

Figure 1: The morphology of the endothelial inner wall surface of the mouse aorta - control sample.